Electron Delocalization in Aminoguanidine: A Computational Study

P. V. Bharatam,* P. Iqbal, A. Malde, and R. Tiwari

Department of Medicinal Chemistry, National Institute of Pharmaceutical Education and Research (NIPER), S.A.S. Nagar (Mohali), 160 062 Punjab, India

Received: February 12, 2004; In Final Form: August 31, 2004

The electronic structure, intramolecular interactions, second-order delocalizations, and C−N rotational barriers in aminoguanidine have been studied using ab initio MO and density functional methods. Isomer **AG1** with intramolecular hydrogen bonding has been found to be the most stable on the potential energy surface, with nine minima. The influences of the basis set, computational method, and solvent effect on relative stabilities of important isomers of aminoguanidine have been studied. Natural Population Analysis (NPA) indicates that amino substitution in guanidine leads to an increased electron delocalization from the center of the NH_2 attachment to the π frame. A strong redistribution of π electron density has been observed in aminoguanidine in relation to guanidine. The protonation energy for aminoguanidine is slightly less than that of guanidine. In protonated aminoguanidine, the π delocalization is more polarized in comparison to that in protonated guanidine. NPA, HOMA, and NICS studies have been carried out to understand electron delocalization in protonated guanidine and aminoguanidine.

Introduction

Aminoguanidine and its derivatives have found applications in both chemical and biological systems. The basic guanidinium functional group is commonly used by proteins and enzymes as an essential recognition unit or catalytic moiety. Several drugs and lead compounds with this moiety have been reported.[1a−l] Aminoguanidine is a drug known to possess extensive pharmacological properties, and it also serves as an important starting material in the synthesis of drugs and enzyme inhibitors.[2a−l] It is known to inhibit diamine oxidase, inducible isoform of nitric oxide synthase (iNOS), etc.[2a−d] It also prevents advancement of diabetic complications such as diabetic angiopathy and retinopathy.[2e,f] Recent studies on the lead optimization of guanidinopropionic acid showed that amino[3] and diamino[4] derivatives are the most potent antihyperglycemic agents. Apart from antidiabetic activity, the aminoguanidine has been implicated as a therapeutic agent for hepatotoxicity,[5a] hypertension,[5b] cardiovascular complications,[5c] microvasculopathy,[5d] diabetic retinopathy,[5e] anticancer therapy,[5f] pulmonary fibrosis,[5g] diabetic neuropathy,[5h] thermal injury,[5i] antiaging activity,[5j] dermatological complications,[5k] etc.

The biological and physiological properties of guanidine derivatives have been attributed to their strong basicity.[6a−d] Under physiological conditions, aminoguanidine is known to exist in the protonated form, which has been confirmed by the cocrystal of iNOS with protonated aminoguanidine.[2d] Aminoguanidine is administered as monohydrochloride or bicarbonate salts. The strong basicity of aminoguanidine is expected to be a result of the stability of its conjugate acid in water.[6a] The internal electron delocalization in aminoguanidine and its redistribution upon protonation or chelation with biometals are expected to be responsible for the observed biological action.[7] It was reported that the presence of an additional NH_2 unit in aminoguanidine is responsible for the reduction in the toxicity of guanidine.[8] To obtain a clear understanding of the electron delocalization in aminoguanidine and its protonated form, it is important to study its electronic structure in detail.

The electronic structure, Y-aromaticity, proton affinity, etc. in guanidines have been studied in detail,[6a−q] but the same characteristics in aminoguanidine are poorly understood. Sapse et al.[9a] reported the HF/6-31G* study on the structural forms of aminoguanidine using planarity constraints. They reported that the C−N rotational barriers are in the range of 11−20 kcal/mol; higher barriers are due to intramolecular hydrogen bonds. Koskinen et al.[10] initially reported the ab initio studies on the endiamine tautomer of aminoguanidine to explain the crystal structure of aminoguanidine monohydrochloride and later[11a,b] extended this work to the study of the tautomers and protonation in aminoguanidine. However, the complete potential energy surface of aminoguanidine was not yet reported. Recently, we found[12a−d] that the observed trends in the C−N barriers in urea, thiourea, and selenourea can be traced to the primary and secondary electron delocalizations in these systems, which in turn are controlled by molecular orbital interactions. In this paper, we explore the electronic structure, electron delocalizations, etc. in aminoguanidine and compare with those of imidamide and guanidine using ab initio MO and DFT methods.

The protonated form of aminoguanidine is more important in both chemical and biochemical conditions. For example, amino substituted guanidines, in their protonated form, are capable of passing through the sodium ion channel in the nerve memberane.[6m] The aminoguanidine free base has not yet been isolated in the pure form. It is known to exist as a monocation or dication in the solid state. The crystal structures of aminoguanidinium monohydrochloride,[10] aminoguanidinium monocation halogenoantimonates(III), and halogenobismuthates(III),[13a] as well as that of aminoguanidinium(2+)aminoguanidinium(1+)hexacholoroantimonate(III)[13b] have been reported. Contradicting reports are available regarding proton affinity and basicity of aminoguanidine. Sapse et al.[9a,b] reported that the proton affinity of aminoguanidine is slightly less than that of guanidine. Koskinen et al.[11a] reported that the proton

* E-mail: pvbharatam@niper.ac.in.

10.1021/jp049366e CCC: $27.50
Published on Web 10/30/2004

affinity of aminoguanidine is significantly larger than that of guanidine, though their potentiometric titrations indicate weaker basicity of aminoguanidine (pK_a in water: 11.5)[11a] in comparison to guanidine (pK_a in water: 13.6).[9b] A high accuracy G2MP2 method is employed in this study to estimate the proton affinity of guanidine and aminoguanidine and to compare electron delocalization in their protonated structures.

Computational Details

Ab initio MO[14a,b] and density functional (DFT)[15a,b] calculations have been carried out using the Gaussian-98 package.[16] Complete optimizations have been performed on guanidine (**Gu**) and aminoguanidine (**AG**), to understand the electronic structure, 1,3-H shift, N−N, C−N and C═N bond rotations, using HF (*E*), B3LYP (*E*),[17a−c] and MP2(full)[18a,b] (*E*) methods at the 6-31+G* basis set. Default convergence criteria (maximum force < 0.0004 a.u., RMS force < 0.0003 a.u., maximum displacement < 0.0018 a.u., and RMS displacement < 0.0012 a.u.) were used for all optimizations. The thermochemical data discussed in this work can probably be slightly influenced by the choice of the convergence criteria, but the trends in the observed data are not expected to be influenced; hence, the default convergence criteria have been employed in this work. Frequencies were computed analytically for all optimized species at all levels to characterize each stationary point as a minimum or a transition state and to estimate the zero point vibrational energies (ZPE). The calculated ZPE values (at 298.15 K) have been scaled by a factor of 0.9153, 0.9806, and 0.9661 for the HF, B3LYP, and MP2(full) levels, respectively.[19] The higher accuracy G2MP2[20] method, which uses less computational time and cost as compared to the G1,[21] G2,[22] and G3[23] methods and is almost as accurate as these highly accurate methods, was employed to obtain more reliable relative energies for all of the structures. Almost all the energy values discussed in this paper are based on G2MP2-free energies (*G*), unless otherwise specifically mentioned (When HF, B3LYP, and MP2(full) results are discussed, the values refer to total energies with ZPE correction (*E*)). The geometrical parameters (bond lengths, bond angles, etc.) discussed in the text are from MP2(full)/6-31+G* level optimized geometries (unless otherwise mentioned). The results obtained on **AG** have been compared with those of hydrazine (H_2N-NH_2), methyleneimine ($H_2C═NH$), imidamide ($H_2N-CH═NH$), guanidine ($(H_2N)_2C═NH$), formaldehyde hydrazone ($H_2C═N-NH_2$), formamide hydrazone ($H_2N-CH═N-NH_2$), and already reported urea ($(H_2N)_2C═O$) systems,[12a] etc.

Atoms in Molecules (AIM)[24] calculations have been performed to estimate intramolecular hydrogen bonding interactions (wherever applicable). The natural bond orbital (NBO) approach[25a,b] has been employed to quantitatively estimate the second-order interactions ($E_{ij} = -2F_{ij}/\Delta E_{ij}$) as energy due to second-order interaction ($\Delta E_{ij} = E_i - E_j$ is the energy difference between the interacting molecular orbitals *i* and *j*; F_{ij} is the Fock matrix element for the interaction between *i* and *j*). The Wiberg bond indices have been evaluated to understand the changes in the bond characteristics as a function of changes in electron delocalization.[25] Solvent effects using the Onsager reaction field model were studied according to the Self-Consistent Reaction Field (SCRF = Dipole) approach[26a−f] for the most stable conformers of **Gu**, **AG**, and their protonated forms with water as a solvent at the HF and B3LYP levels using the 6-31+G* basis set.

The protonated structures of guanidine (**GuP**) and aminoguanidine (**AGP**) were also optimized using the same methods in order to study the protonation energies (eqs 1 and 2) and absolute proton affinity (APA) (eq 3) and to evaluate the electron delocalization of the molecules.

$$E_{prot} = [E(BH^+) - E(B)] + [ZPE(BH^+) - ZPE(B)] \quad (1)$$

$$G_{prot} = G_{298}(BH^+) - G_{298}(B) \quad (2)$$

$$APA = -\Delta H_{298} = H_{298}(B) + H_{298}(H^+) - H_{298}(BH^+) \quad (3)$$

E_{prot} (eq 1)[6n] is the electronic energy of the protonation reaction, G_{prot} (eq 2) is the Gibbs free energy of protonation, and APA is the absolute proton affinity of a molecule (eq 3).[6d] $E(B)$ and $E(BH^+)$ denote the total energies of the base and its conjugate acid, respectively; ZPE is the zero point vibrational energy correction; G_{298} is the free energy at 298.15 K of the free base (B) and its conjugate ionic acid (BH^+); H_{298} is the enthalpy of the free base (B), its conjugate ionic acid (BH^+), and the proton (H^+) at 298.15 K. Equation 1 includes the changes in total energy and in zero point energy, eq 2 includes the changes in total energy, in zero point energy, in thermal energy, and entropy change on going from 0 to 298.15 K, and eq 3 gives the negative of enthalpy change ($-\Delta H_{298}$), which includes the changes in total energy, in zero point energy (ZPE), in vibrational energy on going from 0 to 298.15 K, and in rotational and translational energy, and a work term ($RT = 0.592$ kcal/mol).[14c] For H^+, only the translational energy term is not equal to zero ($H_{298}\ H^+ = 3/2\ RT = 0.899$ kcal/mol at 298.15 K) and a work term ($RT = 0.592$ kcal/mol).[6d] In the present work, E_{prot}, G_{prot}, and APA are calculated using energy, Gibbs free energy, and enthalpy, respectively, obtained at the G2MP2 level of calculation.

Harmonic Oscillator Measure of Aromaticity (HOMA),[27a−h] a geometry-based aromaticity index (HOMA is defined in such a way to give 0 for a model nonaromatic system and 1 for a system where full π electron delocalization occurs) was applied to quantify the extent of π electron delocalization of guanidinium ion and aminoguanidinium ion. HOMA is defined as follows:

$$HOMA = 1 - \frac{\alpha}{n}\sum (d_{opt} - d_i)^2 \quad (4)$$

In this equation, α is the normalization constant (93.52 for CN bonds), n is the number of bonds taken into account, d_{opt} is the optimum bond length that is assumed to be realized when full delocalization of π electrons (1.334 for CN bonds), and d_i are the running bond lengths. The Nucleus Independent Chemical Shift (NICS) index, related to the magnetic properties of the molecule, was applied to quantify the extent of π electron delocalization of the guanidinium ion and the aminoguanidinium ion. It was introduced by Schleyer et al.[28a] and is a new and effective aromaticity index. It is defined as the negative value of absolute shielding computed at a ring center or any other interesting point of the system, determined by the nonweighted mean of the heavy atom coordinates. Aromatic systems are characterized by negative NICS and antiaromatic systems by positive NICS, as discussed in the study of many cyclic systems.[28b−h]

Results and Discussion

Electron Delocalization in Guanidine. The potential energy (PE) surface of guanidine has been studied earlier.[6g,i] However, the second-order interactions and their influence in the electron delocalization have not been described. The important confor-

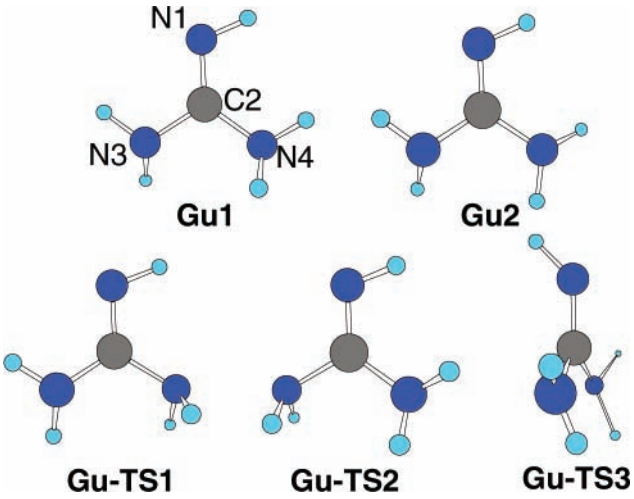

Figure 1. Conformers of Guanidine.

mations of **Gu** and its C−N rotational transition states are given in Figure 1. Complete optimizations at the HF/6-31+G*, B3LYP/6-31+G*, MP2(full)/6-31+G*, and G2MP2 levels indicate that there are two minima (**Gu1** and **Gu2**) on the PE surface of guanidine. The major difference between these two structures is due to the arrangement of hydrogen atoms at N3 and N4: all on one side of the molecular plane as in **Gu2** versus opposite sides as in **Gu1**. **Gu1** is the global minimum; **Gu2** is only about 0.77 kcal/mol higher in energy at the G2MP2 level (Table 1). The two C−NH_2 bonds are unsymmetrical in **Gu1** and possess different partial π strengths as represented by their rotational barriers: 6.82 and 10.84 kcal/mol for the C2−N4 and C2−N3 bonds, respectively (Table 2). The larger C2−N3 rotational barrier may be attributed to the repulsive interactions arising due to the lone pair of electrons on N1 and N3 in **Gu-TS2**, but not due to C2−N3 π strength over C2−N4 π strength. The C−N partial π character in **Gu1** is weaker than that in urea ($(H_2N)_2C{=}O$), thiourea ($(H_2N)_2C{=}S$), and selenourea ($(H_2N)_2C{=}Se$) (as indicated by C−N rotational barriers 6.27, 7.52, 8.81, and 9.44 kcal/mol at the G2 level, respectively).[12a]

There are strong second-order delocalizations in **Gu1** (Table 3). For example, the energy $E^{(2)}$ associated with $n_{N1} \rightarrow \sigma^*_{C2-N4}$ is 23.56 kcal/mol. This negative hyperconjugative interaction causes the elongation of the C2−N4 bond (by about 0.006 Å) in relation to the C2−N3 bond and accounts for the relatively greater $n_{N4} \rightarrow \pi^*_{C2-N1}$ ($E^{(2)}$: 46.09 kcal/mol) π delocalization in comparison to the $n_{N3} \rightarrow \pi^*_{C2-N1}$ delocalization ($E^{(2)}$: 41.58 kcal/mol) (Table 3). The strengths of electron delocalizations observed in **Gu1** are much weaker than those in urea, thiourea, and selenourea ($E^{(2)}$: 56.75, 73.52, and 83.60 kcal/mol, respectively).[12a] This weakness can be mainly attributed to the smaller ΔE between the molecular orbitals involved in the second-order interactions in guanidine as discussed in the case of ureas.[12a] This is also supported by the stronger pyramidalization at N3 and N4 in **Gu1** (sum of angles (φ): 337.0 and 339.7°), in comparison to that in urea (346.6°). The $n_N \rightarrow \pi^*_{C-N}$ electron delocalization in **Gu1** has been found to be stronger than that in imidamide ($E^{(2)}$: 25.83 kcal/mol). The C2=N1 bond rotational path in guanidine is much softer than in simple methyleneimine and imidamide. This is evident from the fact that the C=N rotational barrier in **Gu1** is 21.11 kcal/mol, which is smaller than that of imidamide (24.62 kcal/mol), which is also smaller than that of methyleneimine (27.88 kcal/mol).

Electron Delocalization in Aminoguanidine. *Isomers of Aminoguanidine.* Three types of isomeric process, namely (i) prototropic tautomerism (intramolecular proton transfer), (ii) rotational isomerism (around the C−N and N−X single bonds), and (iii) geometrical E/Z isomerism (around the C=N double bond) are in general observed in guanidine. In the case of aminoguanidine (**AG**), all these processes lead to a total of nine different minima on the PE surface, of which the distinct isomers are **AG1**, **AG2**, and **AG3** (Figure 2), which may be labeled as position isomers. The C−N and N−N rotational processes in **AG2** lead to the minima **AG2-1**, **AG2-2**, and **AG2-3**; a similar process in **AG3** leads to the minima **AG3-1**, **AG3-2**, and **AG3-3**. All the isomers of **AG** are characterized by several second-order interactions, for example, $n_{N1} \rightarrow \sigma^*_{C2-N4}$ negative hyperconjugation. The relatively significant second-order interactions from the N3 and N4 centers will be discussed later.

The isomer **AG1** with amino (NH_2) substitution at the imine nitrogen (N1) has been found to be the most stable. Isomer **AG2** with NH_2 substitution at N3 is about 2.76 kcal/mol less stable than **AG1** at the HF/6-31+G* level. This energy difference increases after including the electron correlation, to 3.99 kcal/mol at the B3LYP/6-31+G* level and to 4.85 kcal/mol at the MP2(full)/6-31+G* level. The higher accuracy G2MP2 method shows the difference to be about 3.37 kcal/mol (Table 4). Similarly, isomer **AG3** with NH_2 substitution at N4 is about 4.30 kcal/mol less stable than **AG1** at the G2MP2 level. The greater stability of **AG1** can be attributed to the intramolecular hydrogen bond in **AG1**, which is absent in both **AG2** and **AG3**. When intramolecular interactions are involved in stabilizing some isomers, it is advisable to use larger basis sets. We have employed 6-311++G(3df,3pd) and aug-cc-pVDZ (with the B3LYP method) to estimate the influence of basis sets on the relative energies of **AG1**, **AG2**, and **AG3** (Table S6). The N5···H8 length of the intramolecular hydrogen bond (2.182 Å at the B3LYP/6-31+G* level) only slightly increased to 2.189 Å (at the B3LYP/6-311++G(3df,3pd) level) and to 2.184 Å (at the B3LYP/aug-cc-pVDZ level). Upon including the diffusion and polarization function on hydrogen, that is, 6-311++G-(3df,3pd), the ΔE (**AG1** − **AG2**) was slightly reduced from 3.97 to 2.91 kcal/mol. Application of the augmented correlation consistent polarized valence double-ζ basis set also showed a reduction in the relative energies among **AG1**, **AG2**, and **AG3** (Table S6). However, the trends in the relative energies remain undisturbed. Hence, we continued the rest of the work with the 6-31+G* basis set. AIM (Atoms in Molecules) calculation on **AG1** (MP2 optimized geometry) showed a N5···H8 bond critical point (between N5 and H8 with $\rho = 0.023\,097$, $\nabla^2\rho = 0.09\,214$, and $\epsilon = 0.5284$) and a ring critical point (for one five-membered ring, H8···N5−N1−C2−N4−H8 and $\rho = 0.02170$), which support the presence of an intramolecular hydrogen bond with an N5···H8 bond length of 2.177 Å. This intramolecular hydrogen bond stabilizes a N−N rotational conformation with *anti* arrangement between the lone pairs across the N−N bond. Such an arrangement happens to be a transition state in hydrazine, in formaldehyde hydrazone as well as in formamide hydrazone.

To understand the influence of polar media on the relative stabilities of **AG1**, **AG2**, and **AG3** and their rotamers, a SCRF study has been carried out with dielectric constant 78.39 (water) at the HF and B3LYP levels using the 6-31+G* level (Table S7 and S8). The results also indicate **AG1** is the most stable isomer in polar media, though the ΔE values between the isomers were reduced. A slight change in the relative stability order (in kcal/mol) has been noticed: **AG1** (0.00) > **AG2** (3.99) > **AG3** (5.11) in the gas phase became **AG1** (0.00) > **AG3** (1.85) > **AG2** (2.40) in the solvent phase at the B3LYP/6-31+G* level. The order of relative stabilities of the rotamers

TABLE 1: Relative Energies (kcal/mol, ZPE Corrected Values that have been Scaled by a Factor of 0.9153, 0.9806, and 0.9661 for HF, B3LYP, and MP2(full) Levels Respectively) of Various Conformers of Guanidine and Aminoguanidine at 298.15 K Using 6-31+G* Basis Set[a]

str.	HF (E)	B3LYP (E)	MP2(full) (E)	G2MP2 (G)	chemical interpretation of the energy data
			guanidine		
Gu1	0.00	0.00	0.00	0.00	global minimum
Gu2	1.20	1.08	1.49	0.77	ΔE between two minima
Gu-TS1	7.55	7.05	7.06	6.82	rot. bar. across C2−N4
Gu-TS2	12.86	12.08	12.40	10.84	rot. bar. across C2−N3
Gu-TS3	23.03	19.14	22.06	21.11	rot. bar. across C2═N1
			N1-aminoguanidine		
AG1	0.00	0.00	0.00	0.00	global minimum
AG1-TS1	10.95	9.33	9.25	7.72	rot. bar. across C2−N3
AG1-TS2	9.15	9.00	9.33	8.78	rot. bar. across C2−N4
AG1-TS3	42.82	32.62	37.92	36.44	rot. bar. across C2═N1
			N3-aminoguanidine		
AG2	0.00	0.00	0.00	0.00	global minimum
AG2-1	0.95	0.81	1.41	1.60	ΔE between two minima
AG2-2	3.79	3.26	3.58	3.34	ΔE between two minima
AG2-3	7.02	6.87	6.90	6.04	ΔE between two minima
AG2-TS1	6.69	5.96	5.96	5.91	rot. bar. across C2−N4
AG2-TS2	15.16	14.40	14.34	13.74	rot. bar. across C2−N3
AG2-TS3	23.09	18.69	21.42	20.51	rot. bar. across C2═N1
			N4-aminoguanidine		
AG3	0.00	0.00	0.00	0.00	global minimum
AG3-1	−0.14	0.25	−0.32	0.67	ΔE between two minima
AG3-2	0.52	0.30	0.83	1.16	ΔE between two minima
AG3-3	2.08	1.67	1.74	2.16	ΔE between two minima
AG3-TS1	11.88	11.16	11.07	10.55	rot. bar. across C2−N3
AG3-TS2	11.13	11.10	10.49	11.01	rot. bar. across C2═N4
			protonated aminoguanidine		
AGP1	0.00	0.00	0.00	0.00	global minimum
AGP2	6.67	6.07	7.42	5.52	ΔE between two minima

[a] *E* is the total energy, *G* is the free energy, rot. bar. is the rotational barrier.

TABLE 2: Barriers to Rotation (kcal/mol) of the Most Stable Conformers of Guanidine (Gu), the Three Major Isomers of Aminoguanidine (AG1, AG2, AG3), and Their Protonated Forms (GuP and AGP1) Obtained at MP2(full)/6-31+G* and G2MP2 Level at 298.15 K[a]

	C═N1		C−N3		C−N4		N−N	
str.	MP2(f) (*E*)	G2MP2 (*G*)	MP2(f) (*E*)	G2MP2 (*G*)	MP2(f) (*E*)	G2MP2 (*G*)	MP2(f) (*E*)	G2MP2 (*G*)
Gu1	22.06	21.11	12.40	10.84	7.06	6.82	-	-
AG1	37.92	36.44	9.25	7.72	9.33	8.78	10.25	8.16
AG2	21.42	20.51	14.34	13.74	5.96	5.91	10.49	9.06
AG3	16.50	15.93	11.38	10.55	10.81	11.01	11.04	9.12
GuP	11.96	13.18	11.96	13.18	11.96	13.18	-	-
AGP1	18.85	18.70	9.78	9.93	16.30	15.79	13.34	11.76

[a] *E* is the total energy, *G* is the free energy.

of **AG2** remains the same in the aqueous phase at the B3LYP/6-31+G* level, with **AG2-1**, **AG2-2**, and **AG2-3** being 0.66, 2.58, and 6.96 kcal/mol less stable than **AG2**, respectively. However, in the case of **AG3**, a slight change in the order of the relative stabilities was observed from **AG3** (0.00) > **AG3-1** (0.25) > **AG3-2** (0.30) > **AG3-3** (1.67) in the gas phase to **AG3** (0.00) > **AG3-3** (0.93) > **AG3-1** (1.15) > **AG3-2** (3.92) in the solvent phase at the B3LYP/6-31+G* level. The observed slight reversal in the relative stabilities of isomers of aminoguanidine under polar conditions may be attributed to the increased number of lone pairs exposed to solvent (For example, three lone pairs of electrons in **AG2** to four lone pairs of electrons in **AG3**).

Isomeric Processes in Aminoguanidine. Prototropic tautomerism is one of the important processes of guanidine and its derivatives.[6c] It can be effectively studied using computational chemistry methods as reported on many basic systems.[29a−k] In the solution phase, this process must have been taking place through a protonated derivative along a bimolecular pathway. However, it is interesting to note the energy barriers involved in the unimolecular 1,3-H shift under gas phase conditions. Among the nine different minima on the PE surface of **AG**, only three different 1,3-H shifts are theoretically possible; they are between **AG2-1** ⇌ **AG1**, **AG3-2** ⇌ **AG3**, and **AG3-3** ⇌ **AG3-1**.[30] The energy barriers for these three 1,3-H shift processes are 36.54, 41.53, and 40.54 kcal/mol, respectively. These barriers are much smaller than the barrier noted for keto−enol tautomerism (56.33 kcal/mol for $H_3C-CHO \leftrightarrow H_2C{=}CHOH$) and imine−enamine tautomerism (61.21 kcal/mol for $H_3C-CH{=}NH \leftrightarrow H_2C{=}CH-NH_2$), but they are similar to that in guanidine (42.00 kcal/mol) and in imidamide (43.93 kcal/mol). The smaller 1,3-H shift barrier in **AG2-1** ⇌ **AG1** indicates that the hydrogen shift from N3 to N1 in **AG2-1** is benefited by the presence of the (N^5H_2) amino group, which induces weakness in the N3−H7 bond due to $n_{N5} \rightarrow \sigma^*_{N3-H7}$ negative hyperconjugation.

The **AG2-1** ⇌ **AG1** 1,3-H shift process is of practical importance since this is the only unimolecular path that helps

TABLE 3: NBO Analysis of the Most Stable Conformers of Guanidine (Gu), the Three Major Isomers of Aminoguanidine (AG1, AG2, AG3), and Their Protonated Forms at the MP2(full)/6-31+G* Level at 298.15 K

		second-order interaction			occupancy	
str.	interaction	$E^{(2)a}$	$E_i - E_j{}^b$	$F_{ij}{}^b$	$\rho n_{(N)}$	$\rho_{\pi^*(C2-N1)}$
Gu1	$n_{N3}-\pi^*_{C2-N1}$	41.58	0.67	0.153	$1.893_{(N3)}$	0.212
	$n_{N4}-\pi^*_{C2-N1}$	46.09	0.68	0.162	$1.892_{(N4)}$	
	$n_{N1}-\sigma^*_{C2-N4}$	23.56	1.22	0.152	$1.939_{(N1)}$	
AG1	$n_{N3}-\pi^*_{C2-N1}$	40.28	0.67	0.152	$1.896_{(N3)}$	0.238
	$n_{N4}-\pi^*_{C2-N1}$	53.22	0.65	0.171	$1.872_{(N4)}$	
	$n_{N1}-\sigma^*_{C2-N4}$	18.22	1.29	0.137	$1.951_{(N1)}$	
	$n_{N5}-\sigma^*_{N4-H8}$	5.50	1.28	0.075	$1.980_{(N5)}$	
AG2	$n_{N3}-\pi^*_{C2-N1}$	46.83	0.65	0.160	$1.870_{(N3)}$	0.222
	$n_{N4}-\pi^*_{C2-N1}$	44.41	0.67	0.159	$1.893_{(N4)}$	
	$n_{N1}-\sigma^*_{C2-N4}$	23.23	1.23	0.151	$1.935_{(N1)}$	
	$n_{N5}-\sigma^*_{C2-N3}$	7.44	1.21	0.085	$1.979_{(N5)}$	
AG3	$n_{N3}-\pi^*_{C2-N1}$	38.16	0.67	0.147	$1.896_{(N3)}$	0.214
	$n_{N4}-\pi^*_{C2-N1}$	51.51	0.66	0.168	$1.868_{(N4)}$	
	$n_{N1}-\sigma^*_{C2-N4}$	23.30	1.23	0.151	$1.939_{(N1)}$	
	$n_{N5}-\sigma^*_{C2-N4}$	8.56	1.20	0.091	$1.975_{(N5)}$	
GuP	$n_{N3}-\pi^*_{C2-N1}$	112.48	0.48	0.220	$1.762_{(N3)}$	0.443
	$n_{N4}-\pi^*_{C2-N1}$	112.49	0.48	0.220	$1.762_{(N4)}$	
AGP1	$n_{N3}-\pi^*_{C2-N4}$	112.35	0.50	0.221	$1.777_{(N3)}$	0.430
	$n_{N1}-\pi^*_{C2-N4}$	109.64	0.50	0.221	$1.742_{(N4)}$	
	$n_{N5}-\sigma^*_{N1-H12}$	9.83	1.19	0.097	$1.967_{(N5)}$	
AGP2	$n_{N3}-\pi^*_{C2-N4}$	107.23	0.49	0.216	$1.767_{(N3)}$	0.446
	$n_{N1}-\pi^*_{C2-N4}$	125.06	0.48	0.230	$1.742_{(N4)}$	
	$n_{N5}-\sigma^*_{C2-N1}$	12.01	1.23	0.108	$1.966_{(N5)}$	

[a] In kcal/mol. [b] In a.u.

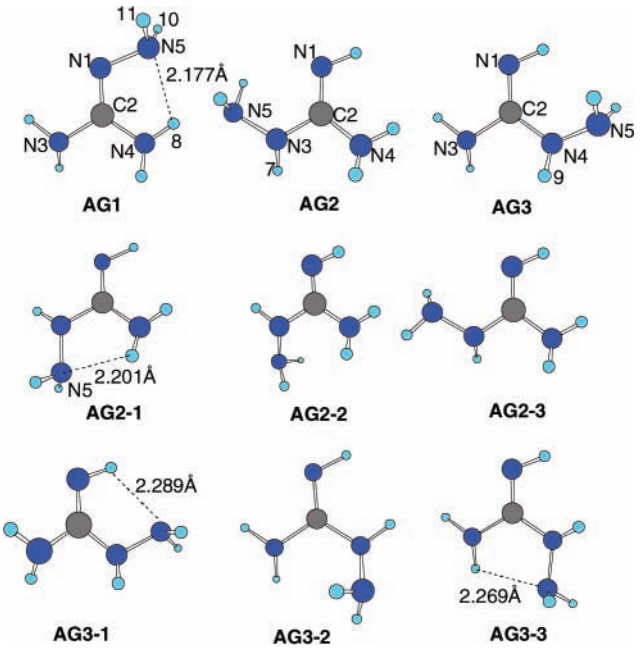

Figure 2. Isomers of Aminoguanidine (the geometric details are given in Table S5).

TABLE 4: Relative Energies (kcal/mol) of the Most Stable Conformers of the Three Major Isomers of Aminoguanidine (AG1, AG2, AG3) Using Different Theoretical Methods at 298.15 K Using 6-31+G* Basis Set

str.	HF (*E*)	B3LYP (*E*)	MP2(full) (*E*)	G2MP2 (*G*)
AG1	0.00	0.00	0.00	0.00
AG2	2.76	3.99	4.85	3.37
AG3	4.09	5.11	6.28	4.30

[a] *E* is the total energy, *G* is the free energy.

in converting all the minima to the global minimum on the PE surface of **AG** (Figure 3 gives a schematic representation of the interconversion of the various isomers of aminoguanidine

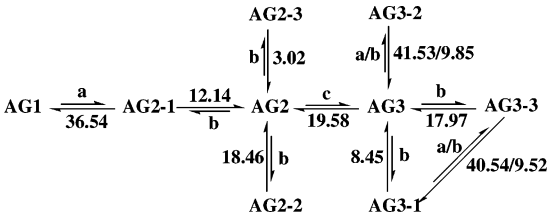

Figure 3. Schematic representation of possible interconversion paths of isomers of aminoguanidine. The energy values (in kcal/mol at G2MP2 level) are barrier for interconversion from higher energy isomer to lower energy isomer. (a) 1,3-H shift barrier, (b) Rotational barrier and (c) E/Z Isomerization barrier.

through different mechanisms.). It is interesting to note that none of the rotational isomers of **AG3** (**AG3**, **AG3-1**, **AG3-2**, and **AG3-3**) can be converted directly to either **AG1** or **AG2** via the 1,3-H shift. It may take place only after *E*/*Z* isomerization from **AG3** to **AG2**, which requires a barrier of 19.58 kcal/mol. The geometrical *E*/*Z* isomers **AG2** and **AG3** were not reported by previous workers,[11a] though slightly less stable rotamers of these two positional isomers were reported. The three minima **AG2-1**, **AG2-2**, and **AG2-3** (Figure 2) are higher in energy than **AG2** by 1.60, 3.34, and 6.04 kcal/mol, respectively (Table 1). The rotational isomers **AG3-1**, **AG3-2**, and **AG3-3** are less stable than **AG3** (Figure 2) by 0.67, 1.16, and 2.16 kcal/mol respectively (Table 1). The order of preference of these isomer remain the same at almost all levels, except that **AG3-1** becomes relatively more stable than **AG3** according to HF and MP2 level calculations (Table 1). Though the observed N5···H(N4) distance is 2.201 Å in **AG2-1**, the N5···H(N1) distance is 2.289 Å in **AG3-1** and the N5···H(N3) distance is 2.269 Å in **AG3-3**, which are all within the range of the hydrogen bond length; AIM calculations do not show any distinct bond critical point or ring critical point corresponding to the presence of an intramolecular hydrogen bond.

Electron Delocalization from N5. One of the important aspects to be addressed in this work is whether the lone pair on N^5H_2 is playing any role in the electron delocalization to the π frame. The structures of **AG1**, **AG2**, and **AG3** do not give any indication of extended conjugation of the lone pair on N5 to the π frame of **AG**. The N−N rotational barriers in **AG1**, **AG2**, and **AG3** respectively are 8.16, 9.06, and 9.12 kcal/mol (Table 2) and all are slightly higher than that in hydrazine (7.80 kcal/mol). The increase in these values can be attributed to the intramolecular hydrogen bond in **AG1**, lone pair (N1)−lone pair (N5) repulsions in **AG2**, and 1,4 repulsions arising due to (N1)H···H(N5) interactions in **AG3**, none of these are due to loss of the N5 lone pair π distribution, indicating that the N5 lone pair is not involved in π delocalization in any of the isomers of **AG**. The lone pair on N5 participates in relatively less prominent interactions as below. In **AG1**, it is involved in $n_{N5} \rightarrow \sigma^*_{N4-H8}$ ($E^{(2)}$: 5.50 kcal/mol) anomeric interaction, contributing to the intramolecular hydrogen bond; in **AG2** it is involved in $n_{N5} \rightarrow \sigma^*_{C2-N3}$ ($E^{(2)}$: 7.44 kcal/mol) negative hyperconjugative interaction, and in **AG3** it is involved in $n_{N5} \rightarrow \sigma^*_{C2-N4}$ ($E^{(2)}$: 8.56 kcal/mol) negative hyperconjugative interaction (Table 3). The NPA charges (Table S9) obtained in all of the isomers showed reduction in the negative charge at the amino substituted nitrogen center, while the other atoms showed similar charge distribution as in the case of guanidine.

C−N Rotational Process in Aminoguanidine. Electron delocalization in **AG1** can be understood as a function of C2−N3 and C2−N4 (Figure 4) bond rotations, which are 7.72 and 8.78 kcal/mol, respectively. NBO analysis shows strong electron delocalization from N3 ($n_{N3} \rightarrow \pi^*_{C2-N1}$: $E^{(2)}$: 40.28 kcal/mol)

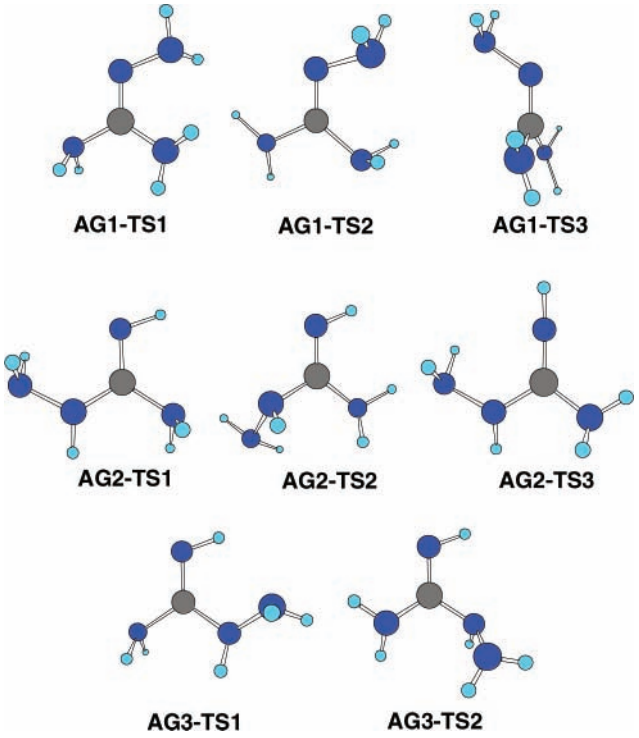

Figure 4. Rotational transition states of **AG1**, **AG2** and **AG3**.

and from N4 ($n_{N4} \rightarrow \pi^*_{C2-N1}$: ($E^{(2)}$: 53.22 kcal/mol) (Table 3), which indicates stronger partial C2−N4 π strength in comparison to C2−N3 bond. Three major points became evident while comparing the C−N rotational processes in **Gu1** and **AG1**: (i) the C2−N3 rotational barrier decreased from 10.84 kcal/mol in **Gu1** to 7.72 kcal/mol in **AG1**, (ii) the C2−N4 rotational barrier increased from 6.82 to 8.78 kcal/mol, and (iii) the C2−N1 rotational barrier increased significantly from 21.11 kcal/mol in **Gu1** to 36.44 kcal/mol in **AG1** (Table 2). This comparison indicates that there is strong redistribution of π electron density in **AG1** in relation to **Gu1**. This is supported by the slight decrease (41.58 to 40.58 kcal/mol) in $n_{N3} \rightarrow \pi^*_{C2-N1}$ delocalization and a large increase (46.09 to 53.22 kcal/mol) for the $n_{N4} \rightarrow \pi^*_{C2-N1}$ delocalization from **Gu1** to **AG1** (Table 3).

During C2−N3 rotation in **AG1**, **AG1-TS1** is the rotational transition state. **AG1-TS1** is characterized by (i) the lack of $n_{N3} \rightarrow \pi^*_{C2-N1}$, which is replaced by a weaker delocalization $n_{N3} \rightarrow \sigma^*_{C2-N4}$ negative hyperconjugative delocalization and is also characterized by (ii) repulsions between the lone pairs on N1 and N3, which are present in **Gu-TS2**. However, **AG1-TS1** is additionally characterized by (iii) breaking of the intramolecular hydrogen bond, which is replaced by $n_{N5} \rightarrow \pi^*_{C2-N1}$ delocalization. This compensates the energy loss upon C2−N3 rotation and causes a decrease in the C2−N3 rotational barrier. The energy compensation may be estimated to be about 1.78 kcal/mol as a function of the energy difference between the C2−N3 rotational structure with 3N-6 and 3N-7 degrees of freedom (i.e., unrestricted and restricted N1−N5 rotation during C2−N3 rotation). The C2−N4 rotational process in **AG1** through **AG1-TS2** is characterized by (i) a loss in intramolecular hydrogen bond, (ii) a loss of $n_{N4} \rightarrow \pi^*_{C2-N1}$ delocalization, and (iii) a gain in the $n_{N4} \rightarrow \sigma^*_{C2-N1}$ anomeric π strength together contribute to the C2−N4 rotational barrier. The C2═N1 rotational path in **AG1** through the transition state **AG1-TS3** is 36.44 kcal/mol (Table 2). This is larger than in methyleneimine (27.88 kcal/mol), imidamide (24.62 kcal/mol), and guanidine (21.11 kcal/mol), indicating that the geometrical isomerism through the transition state **AG1-TS3** is not an allowed path in aminoguanidine **AG1**.

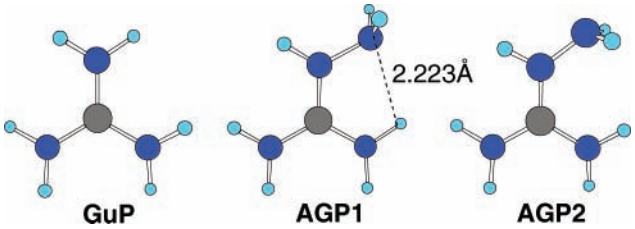

Figure 5. Protonated conformers of guanidine and aminoguanidine.

TABLE 5: Protonation Energies (E_{prot}, G_{prot}) and Absolute Proton Affinity (APA) of Guanidine and Aminoguanidine at G2MP2 Level of Calculations (kcal/mol) at 298.15 K

str.	E_{prot}	G_{prot}	APA
Gu	−234.93	−235.77	235.68
AG1	−234.84	−235.14	235.94

An analysis of electron delocalization in **AG2** and **AG3** indicates that the point of attachment of the NH_2 group plays an important role. In **AG2**, delocalization of the N3 lone pair is relatively greater, whereas in **AG3**, delocalization of the N4 lone pair is greater. For example, in **AG2** the second-order energy due to $n_{N3} \rightarrow \pi^*_{C2-N1}$ delocalization is 46.83 kcal/mol (an increase from 41.58 kcal/mol in **Gu1**) and $n_{N4} \rightarrow \pi^*_{C2-N1}$ delocalization is 44.11 kcal/mol (an decrease from 46.09 kcal/mol in **Gu1**) (Table 3). The C2−N3 and C2−N4 bond rotational barriers (Table 2) also support the above observation. An opposite trend was observed in **AG3**.

Electron Delocalization in Protonated Guanidine and Aminoguanidine. The electronic energy change of protonation (E_{prot}), Gibbs free energy change of protonation (G_{prot}), and absolute proton affinity (APA) values of **Gu** estimated using the G2MP2 method (using eqs 1, 2, and 3) are −234.93, −235.77, and 235.68 kcal/mol, respectively (Table 5). The calculated APA value of 235.68 kcal/mol falls within the expected range (235−236 kcal/mol at the G2 level[6d]) and the FT-ICR estimate of 235.7 kcal/mol.[6q] The improved electron delocalization upon protonation has been shown to be the reason for the high proton affinity. The C−N rotational barrier in **GuP** has been estimated to be 13.18 kcal/mol at the G2MP2 level (Table 2).

The estimated APA of **AG1** at the HF/6-31+G* level (eq 1) is 235.02 kcal/mol. This value is reduced to 228.54 and 225.15 kcal/mol upon including electron correlation at the B3LYP/6-31+G* and MP2(full)/6-31+G* levels (eq 1), respectively (Table S13). A similar correlation effect is also observed in the case of **Gu**, where at the HF/6-31+G* level the value of APA is 234.11 kcal/mol, which upon inclusion of electron correlation at the B3LYP/6-31+G* and MP2(full)/6-31+G* levels is reduced to 228.24 and 224.29 kcal/mol, respectively (Table S13). At the higher accuracy G2MP2 method, the estimated E_{prot}, G_{prot}, and APA of **AG1** are −234.84, −235.14, and 235.94 kcal/mol, respectively. These values are very close to the corresponding values of guanidine, indicating that the Lewis basicity of aminoguanidine is quite comparable to that of guanidine.

All the isomers of aminoguanidine lead to the same protonated aminoguanidine **AGP**, which may exist in either of the two conformational minima **AGP1** and **AGP2** (Figure 5). The difference between the two structures arise due to rotation across the N−N bond. **AGP1** is characterized by the intramolecular hydrogen bond N5···H8 (2.223 Å), which is confirmed by the presence of a bond critical point (between N5 and H8 with ρ =

0.021 357, $\nabla^2\rho = 0.08889$, and $\epsilon = 0.5794$) and a ring critical point (for one five-membered ring, H8···N5−N1−C2−N4−H8 and $\rho = 0.02029$) as shown by AIM calculations. **AGP1** is characterized by $n_{N5} \rightarrow \sigma^*_{N1-H12}$ second-order interactions, and **AGP2** is characterized by $n_{N5} \rightarrow \sigma^*_{C2-N1}$ second-order interactions (Table 3). The energy difference between the two conformers is 5.52 kcal/mol. The N−N rotational barrier in **AGP1** is about 11.76 (Table 2) kcal/mol at the G2MP2 level, which is about 3.94 kcal/mol higher in energy than the rotational barrier (7.80 kcal/mol) in hydrazine.

The C2═N1, C2−N3, and C2−N4 rotational barriers in **AGP1** are 18.70, 9.93, and 15.79 kcal/mol (Table 2), respectively. This indicates that unlike in **GuP**, where all of the C−N partial double bonds become practically equivalent after protonation, the C−N bonds in **AGP** are highly polarized. The C2═N1 rotation barrier (18.70 kcal/mol) in **AGP1** is much smaller than that in **AG1** (36.44 kcal/mol), but the C2−N3 and C2−N4 rotational barriers show an increase upon protonation. This trend is according to the expectations based on increased delocalization upon protonation. The higher barriers for the C2═N1 and C2−N4 rotations in **AGP1** in comparison to **GuP** are due to the intramolecular hydrogen bond.

The bond characteristics and the extent of π delocalization in **GuP** and **AGP1** can be estimated using several indices: Wiberg bond indices represent the bond characteristics of a system while the geometry based aromaticity index, HOMA, and the magnetic property based aromaticity index, NICS, can be used to understand delocalization characteristics. The Wiberg bond indices for the C2═N1, C2−N3, and C2−N4 bonds are all equivalent to 1.28 for **GuP** and 1.23, 1.27, and 1.31, respectively, for **AGP1** (Table S11). This supports our earlier observation that the electron delocalization in **AGP1** is more polarized compared to **GuP**. The calculated HOMA (eq 3) value for **GuP** is 0.999, while Krygowski et al.[27h] reported HOMA = 1.011 for guanidinium salts. This clearly implies that the delocalization of π electrons in the $C(N)_3$ moiety in guanidine is very high (for benzene, HOMA = 0.979). The evaluated HOMA value for **AGP1** is 0.998 (Table S14), which is comparable to that of the guanidinium ion. The NICS values calculated for the guanidinium ion and the aminoguanidinium ion, respectively, are −44.1 ppm and −37.6 ppm, much larger than that of benzene (−9.7 ppm) (Table S14). Though the numerical values cannot be taken as a measure of relative strengths of delocalization, the negative NICS values confirm strong delocalization in **GuP** as well as in **AGP1**. Since the $C(N)_3$ moiety is intact in aminoguanidine, the substitution of an amino group does not perturb the existing strong π electron delocalization of the guanidinium moiety.

The NPA charges obtained for the **GuP** suggest that the charge is equally distributed across the molecule. The positive charge concentration on the hydrogens is much larger than that at the central carbon. This is similar to the observation on **AGP**; hence, its polarizability in aqueous conditions is also expected to be as high as in guanidine.[6d,o] This may enable the peripheral protons in the aminoguanidinium ion to participate in electrostatic interactions or hydrogen bond interactions in the solution phase more favorably. In the solvent phase, the relative energy order between **AGP1** and **AGP2** is altered, making the latter more stable in polar media (water) with a difference of −5.40 kcal/mol between the two conformers at the B3LYP/6-31+G* level. This reversal of the relative energy order can be explained on the basis of breaking of the intramolecular hydrogen bonding and also on the availability of the lone pair on the N5 atom for solvent interactions in the case of **AGP2**. From the structure analysis of the cocrystal of the protonated aminoguanidine and iNOS,[2d] it has been observed that the protonated aminoguanidine is present in the distal pocket of the oxygenase domain in iNOS. The guanidino nitrogen and the amino nitrogen of the protonated aminoguanidine form a hydrogen bond with the carboxyl oxygen atom of Glu371, and both the terminal guanidino nitrogens form hydrogen bonds with Trp366 peptide carbonyl. These interactions indicate that the protonated aminoguanidine adopts the orientation similar to that of **AGP2** inside the active site of the oxygenase domain of iNOS, which corroborates the above solvent analysis.

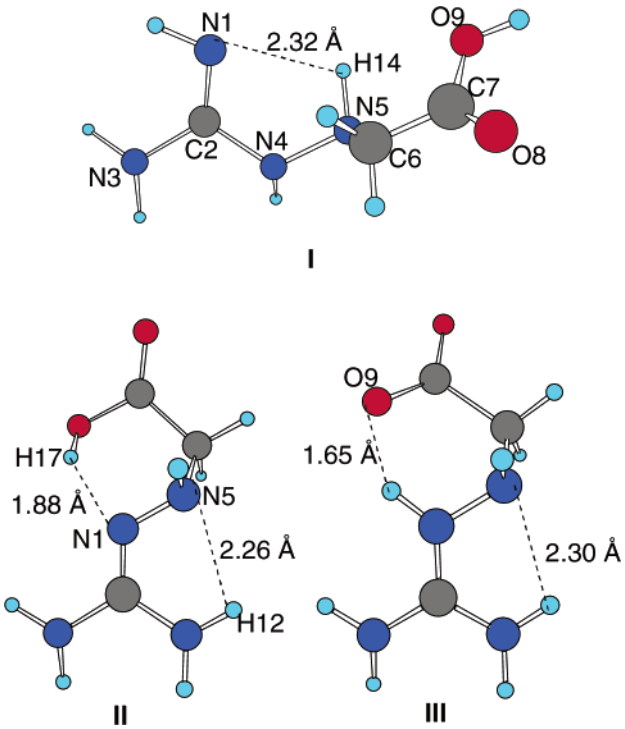

Figure 6. Conformations of aminoguanidinoacetic acid.

The above study on the electronic structure of aminoguanidine can be extended to understand the electronic structure of its derivatives. One important requirement is to find the structure of aminoguanidinoacetic acid (**AGAA**), which was shown to exist as a zwitter ion.[5] A major question is whether **AGAA** is a derivative of **AG1** or **AG2**. Earlier reports represented **AGAA** as a derivative of **AG2** (**I**) (Figure 6). If it were to be a derivative of **AG1** (the most stable isomer of aminoguanidine), it should have been represented as in **II**, which is also convenient for the zwitter ion (**III**) formation. Our calculations suggested that **II** is the proper representation of **AGAA**. Structure **II** is also characterized by two intramolecular hydrogen bonds (N1···H17: 1.88 Å and N5···H12: 2.26 Å). Structure **II** is more stable than **I** by 5.09 kcal/mol at the HF/6-31+G* level. The ΔE between **II** and **III** in the gas phase has been found to be 15.46 kcal/mol at the HF/6-31+G* level, favoring **II**. In the solvent phase, the relative energy order between structure **II** and structure **III** of aminoguanidinoacetic acid is reversed, that is, the zwitter ion structure is more stable in water than structure **II** by 16.80 kcal/mol at the HF/6-31+G* level. However, structure **I** is still the least stable, with an energy difference of 29.86 kcal/mol relative to structure **III**. This clearly suggests that the antidiabetic lead compounds based on aminoguanidine are actually derivatives of **AG1**, but not of **AG2** or **AG3**.

Conclusions

Ab initio MO and density functional calculations on aminoguanidine showed that there are three major isomers and nine conformational minima on the PE surface. The isomer **AG1** is the most stable and is characterized by an intramolecular hydrogen bond. The isomers **AG2** and **AG3** are about 3.37 and 4.30 kcal/mol less stable than **AG1**, respectively. Interconversion between the minima is possible only through some specific pathways, as shown in Figure 3. The three major isomerization paths, namely prototropic tautomerism, rotational isomerism, and E/Z isomerism, are all possible in aminoguanidine as in guanidine, but these processes take place along well-defined routes in aminoguanidine rather than among all isomers. For example, neither isomer **AG3** nor any of its C−N rotamers can show prototropic tautomerization to **AG1**. The π electron delocalization in aminoguanidine is comparatively different from that of guanidine, as indicated by differences in the C−N rotational barriers and the NPA second-order electron distributions. The electronegativity of the substituent (NH_2) and its lone pair participation in intramolecular interactions are responsible for the observed differences. For example, the second-order delocalization increases from the location of NH_2 substitution in guanidine. Polar solvents may cause a slight change in the relative stabilities of various isomers; the greater the number of electron lone pairs exposed to solvent, the greater is the influence of polar solvents. The absolute proton affinity of aminoguanidine is 235.94 kcal/mol, only slightly greater than that of guanidine (235.68 kcal/mol). The increase in the electron delocalization upon protonation is similar in guanidine and in aminoguanidine. An extension of similar calculations on the derivatives of aminoguanidines can be helpful in predicting their accurate structures.

Acknowledgment. The authors acknowledge the financial support from the Council of Scientific and Industrial Research (CSIR), New Delhi. The authors thank the reviewers for a thorough evaluation and valuable suggestions for the improvement. The authors also thank Dr. B. Kiran, WSU, Pullman, United States, for constructive discussion.

Supporting Information Available: Tables S1−S4 containing the ZPE corrected absolute energy data of various systems, the geometrical parameters (Table S5), basis set effect (Table S6), solvation energies (Tables S7 and S8), 1,3-H shift barriers (Table S9), NPA group charges (Table S10), Wiberg bond indices (Table S11), protonation energies (Table S12) and HOMA and NICS (Table S13) for various systems. This material is available free of charge via the Internet at http://pubs.acs.org.

References and Notes

(1) (a)Watanabe, C. K. *J. Biol. Chem*. **1918**, *33*, 253. (b) Creutzfeldt, W.; Söling, H. D. Springer: Berlin 1961; 94. (c) Alsever, R. N.; Georg, R. H.; Sussman, K. E. *Endocrinology* **1970**, *86*, 332. (d) Aynsley-Green, A.; Alberti, K. G. *Horm. Metab. Res*. **1974**, *6*, 115. (e) Alberti, K. G. M. M.; Woods, H. F.; Whalley, M. F. *Europ. J. Clin. Invest*. **1973**, *3*, 208. (f) Schatz, H.; Katsilambros, N.; Nierle, C.; Pfeiffer, E. E. *Diabetologia* **1972**, *8*, 402. (g) Minot, A. S.; Dodd, K.; Riven, S. S. *JAMA J. Am. Med. Assoc*. **1939**, *113*, 553. (h) Ishikawa, T.; Isobe, T. *Chem.—Eur. J*. **2002**, *8*, 553. (i) Palagiano, E.; De Marino, S.; Minale, L.; Riccio, R.; Zollo, F.; Iorizzi, M.; Carré, J. B.; Debitus, C.; Lucarain, L.; Provost, J. *Tetrahedron* **1995**, *51*, 3675. (j) Eriks, J. Ch.; von der Goot, H.; Sterk, G. J.; Timmerman, H. *J. Med. Chem*. **1992**, *35*, 3239. (k) Mayr, L. M.; Schmid, F. X. *Biochemistry* **1993**, *32*, 7994. (l) Zheng, Y.-J.; Ornsteun R. L. *J. Am. Chem. Soc*. **1996**, *118*, 11237.

(2) (a) Elo, H. *Bis*(amidinohydrazones) ["*bis*(guanylhydraones)"] as antineoplastic agents. Chemical and biochemical studies. Ph.D. Dissertation, University of Helsinki, Department of Biochemistry, 1989, and references therein. (b) Corbett, J. A.; Tilton, R. G.; Chang, K.; Hasan, K. S.; Ido, Y.; Wang, J. L.; Sweetland, M. A.; Lancaster, J. R., Jr.; Williamson, J. R.; Mcdaniel, M. L. *Diabetes* **1992**, *41*, 552. (c) Tilton, R. G.; Chang, K.; Hasan, K. S.; Smith, S. R.; Petrash, J. M.; Misko, T. P.; Murray, W. M.; Currie, M. G.; Corbett, J. A.; Mcdaniel, M. L.; Unanue, E. R. *J. Immunol*. **1993**, *150*, 231. (d) Crane, B. R.; Arvai, A. S.; Gachhui, R.; Wu, C.; Ghosh, D. K.; Getzoff, E. D.; Stuehr, D. J.; Tainer, J. A. *Science* **1997**, *278*, 425. (e) Brownlee, M. *Diabetes Care* **1992**, *15*, 1835. (f) Osicka, T. M.; Yu, Y.; Lee, V.; Pangiotopoulos, S.; Kemp, B. E.; Jerums, G. *Clin. Sci*. **2001**, *100*, 249. (g) Osicka, T. M.; Kiriazis, Z.; Pratt, L. M.; Jerums, G.; Comper, W. D. *Diabetologia* **2001**, *44*, 230. (h) Unlucerci, Y. M. Y.; Kocak, H.; Seferoglu, G.; BekpInar, S. *Pharmacol. Res*. **2001**, *44*, 95. (i) Unlucerci, Y. M. Y.; BekpInar, S.; Seferoglu, G. *Acta Diabetol*. **2000**, *37*, 71. (j) Kelly, D. J.; Gilbert, R. E.; Cox, A. J.; Soulis, T.; Jerums, G.; Cooper, M. E. *J. Am. Soc. Nephrol*. **2001**, *12*, 2098. (k) Rong, J.; Qiu, H.; Wang, S. *Chin. Med. J. (Beijing Engl. Ed.)* **2000**, *113*, 1087. (l) Brown, C. D.; Zhao, Z. H.; Thomas, L. L.; de Groof, R.; Friedman, E. A. *Am. J. Kidney Diseases* **2001**, *38*, 1414.

(3) Larsen, S. D.; Connell, M. A.; Cudahy, M. M.; Evans, B. R.; May, P. D.; Meglasson, M. D.; O'Sullivan, T. J.; Schostarez, H. J.; Sih, J. C.; Stevens, F. C.; Tanis, S. P.; Tegley, C. M.; Tucker, J. A.; Vaillancourt, V. A.; Vidmar, T. J.; Watt, W.; Yu, J. H. *J. Med. Chem*. **2001**, *44*, 1217.

(4) Vaillancourt, V. A.; Larsen, S. D.; Tanis, S. P.; Burr, J. E.; Connell, M. A.; Cudahy, M. M.; Evans, B. R.; Fischer, P. V.; May, P. D.; Meglasson, M. D.; Robinson, D. D.; Stevens, F. C.; Tucker, J. A.; Vidmar, T. J.; Yu, J. H. *J. Med. Chem*. **2001**, *44*, 1231.

(5) (a) Alam, K.; Nagi, M. N.; Al-Shabanah, O. A.; Al-Bekairi, A. M. *J. Biochem. Mol. Toxicol*. **2001**, *15*, 317. (b) Hong, H.-J.; Shin, H.; Yen, M.-H. *Br. J. Pharmacol*. **2000**, *131*, 631. (c) Doursont, M.-F.; Davidson, E. M.; Szmuch, P.; Liang, Y. Y.; Chelly, J. E. *Portland Press Proceedings* **2001**, *16 (Biology of Nitric Oxide, Part 7)*, 189. (d) Shostak, A.; Wajsbrot, V.; Gotloib, L. *Microvasc. Res*. **2001**, *61*, 166. (e) Du, Y.; Smith, M. A.; Miller, C. M.; Kern, T. S. *J. Neurochem*. **2002**, *80*, 771. (f) Rao, C. V.; Indranie, C.; Simi, B.; Manning, P. T.; Connor, J. R.; Reddy, B. S. *Cancer Res.* **2002**, *62*, 165. (g) de Rezende, M. C.; Martinez, J. A. B.; Capelozzi, V. L.; Simoes, M. J.; Beppu, O. S. *Fundam. Clin. Pharmacol*. **2000**, *14*, 561. (h) Gorlach, C.; Hartobagyi, T.; Hartobagyi, S.; Benyo, Z. *Restor. Neurol. Neurosci*. **2000**, *17*, 71 (i) Inoue, H.; Ando, K.; Wakisaka, N.; Matsuzaki, K.-i.; Aihara, M.; Kumagai, N. *Nitric Oxide* **2001**, *5*, 334. (j) Cantini, C.; Kieffer, P.; Corman, B.; Liminana, P.; Atkinson, J.; Lartaud-Ldjouadiene, I. *Hypertension* **2001**, *38*, 943. (k) Schreiner, V.; Blatt, T.; Schmidt, M.; Staeb, F. PCT Int. Appl. WO 02/26206 (Cl. A61K7/48), 2002.

(6) (a) Hannon, C. L.; Anslyn, E. V. *Bioorganic Chemistry Frontiers*; Dugas, H., Ed.; Springer-Verlag: 1993; Vol. III, p 193. (b) *The Chemistry of Amidines and Imidates*; Patai, S., Ed.; Wiley: Chichester, 1975; Vol. 1. (c) *The Chemistry of Amidines and Imidates*; Patai, S., Rapport, Z., Eds.; Wiley: Chichester, 1991; Vol. 2. (d) Raczynska, E. D.; Cyrañski, M. K.; Gutowski, M.; Rak, J.; Gal, J.-F.; Maria, P.-C.; Darowska, M.; Duczmal, K. *J. Phys. Org. Chem*. **2003**, *16*, 91. (e) *The Chemistry of Guanidine*; American Cyanamid Co.: Wayne, NJ, 1950. (f) Gund, P. *J. Chem. Educ*. **1972**, *49*, 100. (g) Gobbi, A.; Frenking, G. *J. Am. Chem. Soc*. **1993**, *115*, 2362. (h) Caminiti, R.; Pieretti, A.; Bencivenni, L.; Ramondo, F.; Sanna, N. *J. Phys Chem*. **1996**, *100*, 10928. (i) Wiberg, K. B.; Rush, D. J. *J. Am. Chem. Soc*. **2001**, *123*, 2038. (j) Wiberg, K. B.; Rablen, P. R. *J. Am. Chem. Soc*. **1995**, *117*, 2201. (k) Wiberg, K. B.; Breneman, C. M. *J. Am. Chem. Soc*. **1992**, *114*, 831. (l) Wiberg, K. B. *J. Am. Chem. Soc*. **1990**, *112*, 4177. (m) Peeters, D.; Lewy, G.; Wilante, C. *J. Mol. Struct*. **1997**, *416*, 21. (n) Maksic, Z. B.; Kovacevic, B. *J. Org. Chem*. **2000**, *65*, 3303. (o) Amekraz, B.; Tortajada, J.; Morizur, J.-P.; Gonzalez, A. I.; Mo, O.; Yanez, M.; Leito, I.; Maria, P.-C.; Gal, J.-F. *New J. Chem*. **1996**, *20*, 1011. (p) Hille, B. *J. Gen. Physiol*. **1972**, *59*, 637. (q) Hunter, E. P.; Lias, S. G. *J. Phys. Chem. Ref. Data* **1998**, *27*, 431, http://webbook.nist.org.

(7) Price, D. L.; Rhett, P. M.; Thorpe, S. R.; Baynes, J. W. *J. Biol. Chem*. **2001**, *276*, 48967.

(8) (a) Thiele, J. *Ann*. **1892**, *270*, 1. (b) Lieber, E.; Smith, G. B. L. *Chem. Rev*. **1939**, *25*, 213.

(9) (a) Sapse, A. M.; Snyder, G.; Santoro, A. V. *J. Phys. Chem*. **1981**, *85*, 662. (b) Sapse, A. M.; Snyder, G.; Santoro, A. V. *Int. J. Quantum Chem*. **1981**, *20*, 755.

(10) Koskinen, J. T.; Koskinen, M.; Mutikainen, I.; Mannfors, B.; Elo, H. *Z. Naturforsch*. **1996**, *51b*, 1771.

(11) (a) Koskinen, J. T.; Koskinen, M.; Mutikainen, I.; Tilus, P.; Mannfors, B.; Elo, H. *Z. Naturforsch*. **1997**, *52b*, 1259. (b) Koskinen, J. T. *Z. Naturforsch*. **1998**, *53b*, 386.

(12) (a) Bharatam, P. V.; Moudgil, R.; Kaur, D. *J. Phys. Chem*. **2003**, *107*, 1627. (b) Bharatam, P. V.; Uppal, P.; Amita, Kaur, D. *J. Chem. Soc., Perkin Trans*. **2000**, *2*, 43. (c) Bharatam, P. V.; Amita, Kaur, D. *J. Phys. Org. Chem*. **2003**, *16*, 183. (d) Moudgil, R.; Bharatam, P. V.; Kaur, R.; Kaur, D. *Proc. Ind. Acad. Sci. (Chem. Sci.)* **2002**, *114*, 223.

(13) (a) Davidovich, R. L.; Logvinova, V. B.; Tkachev, V. V.; Atovmyan, L. O. *Koord. Khim*. **1995**, *21*, 819. (b) Bujak, M.; Osadczuk, P.; Zaleski, J. *Acta Crystallogr*. **2001**, *C57*, 388.

(14) (a) Pople, J. A.; Beveridge, D. L. *Approximate Molecular Orbital Theory*; McGraw-Hill: New York, 1970. (b) Hehre, W. J.; Radom, L.;

Schleyer, P. v. R.; Pople, J. A. *Ab initio Molecular Orbital Theory*; Wiley: New York, 1985. (c) http://Gaussian.com/g_whitepap/thermo.htm.

(15) (a) Parr, R. G.; Yang, W. *Density Functional Theory of Atoms and Molecules*; Oxford University Press: New York, 1989. (b) Bartolotti, L. J.; Fluchick, K. In *Reviews in Computational Chemistry*; Lipkowitz, K. B., Boyd, D. B., Eds.; VCH Publishers: New York, 1996; Vol. 7, 187.

(16) Frisch, M. J.; Trucks, G. W.; Schlegel, H. B.; Scuseria, G. E.; Robb, M. A.; Cheeseman, J. R.; Zakrzewski, V. G.; Montgomery, J. A.; Stratmann, R. E., Jr.; Burant, J. C.; Dapprich, S.; Millam, J. M.; Daniels, A. D.; Kudin, K. N.; Strain, M. C.; Farkas, O.; Tomasi, J.; Barone, V.; Cossi, M.; Cammi, R.; Mennucci, B.; Pomelli, C.; Adamo, C.; Clifford, S.; Ochterski, J.; Petersson, G. A.; Ayala, P. Y.; Cui, Q.; Morokuma, K.; Malick, D. K.; Rabuck, A. D.; Raghavachari, K.; Foresman, J. B.; Cioslowski, J.; Ortiz, J. V.; Baboul, A. G.; Stefanov, B. B.; Liu, G.; Liashenko, A.; Piskorz, P.; Komaromi, I.; Gomperts, R.; Martin, R. L.; Fox, D. J.; Keith, T.; Al-Laham, M. A.; Peng, C. Y.; Nanayakkara, A.; Gonzalez, C.; Challacombe, M.; Gill, P. M. W.; Johnson, B.; Chen, W.; Wong, M. W.; Andres, J. L.; Gonzalez, C.; Head-Gordon, M.; Replogle, E. S.; Pople, J. A. *Gaussian-98*, set of programs; Gaussian, Inc.: Pittsburgh, PA, 1998.

(17) (a) Becke, A. D. *J. Chem. Phys*. **1993**, *98*, 5648. (b) Lee, C.; Yang, W.; Parr, R. G. *Phys. Rev*. **1988**, *37B*, 785. (c) Perdew, J. P.; Wang, Y. *Phys. Rev*. **1992**, *45B*, 13244.

(18) (a) Moller, C.; Plesset, M. S. *Phys. Rev*. **1934**, *46*, 618. (b) Krishan, R.; Frisch, M. J.; Pople, J. A. *J. Chem. Phys*. **1980**, *72*, 4244.

(19) Scott, A. P.; Radom, L. *J. Phys. Chem*. **1996**, *100*, 16502.

(20) Curtiss, L. A.; Raghavachari, K.; Pople, J. A. *J. Chem. Phys*. **1993**, *98*, 1293.

(21) (a) Pople, J. A.; Head-Gordon, M.; Fox, D. J.; Raghavachari, K.; Curtiss, L. A. *J. Chem. Phys*. **1989**, *90*, 5622. (b) Curtiss, L. A.; Jones, L.; Trucks, G. W.; Raghavachari, K.; Pople, J. A. *J. Chem. Phys*. **1990**, *93*, 2537.

(22) Curtiss, L. A.; Raghavachari, K.; Trucks, G. W.; Pople, J. A. *J. Chem. Phys*. **1991**, *94*, 7221.

(23) Curtiss, L. A.; Raghavachari, K.; Redfern, P. C.; Rassolov, V.; Pople, J. A. *J. Chem. Phys*. **1998**, *109*, 7764.

(24) Bader, R. F. W. *Atoms in Molecules: A Quantum Theory*; Oxford University Press: Oxford, 1990.

(25) (a) Reed, A. E.; Weinstock, R. B.; Wienhold, F. *J. Chem. Phys*. **1985**, *83*, 735. (b) Reed, A. E.; Wienhold, F.; Curtiss, L. A. *Chem. Rev*. **1988**, *88*, 899.

(26) (a) Onsager, L. *J. Am. Chem. Soc*. **1936**, *58*, 1486. (b) Kirkwood, J. G. *J. Chem. Phys*. **1934**, *2*, 351. (c) Wong, M. W.; Frisch, M. J.; Wiberg, K. B. *J. Am. Chem. Soc*. **1991**, *113*, 4776. (d) Wong, M. W.; Wiberg, K. B.; Frisch, M. J. *J. Am. Chem. Soc*. **1992**, *114*, 523. (e) Wong, M. W.; Wiberg, K. B.; Frisch, M. J. *J. Chem. Phys*. **1991**, *95*, 8991. (f) Wong, M. W.; Wiberg, K. B.; Frisch, M. J. *J. Am. Chem. Soc*. **1992**, *114*, 1645.

(27) (a) Krygowski, T. M. *J. Chem. Inf. Comput. Sci*. **1993**, *33*, 70. (b) Cyrañski, M.; Krygowski, T. M. *J. Chem. Inf. Comput. Sci*. **1996**, *36*, 1142. (c) Krygowski, T. M.; Cyrañski, M. *Tetrahedron* **1996**, *52*, 1713. (d) Krygowski, T. M.; Cyrañski, M. *Tetrahedron* **1996**, *52*, 10255. (e) Krygowski, T. M.; Cyrañski, M. K.; Czarnocki, Z.; Häfelinger, G.; Katritzky, A. R. *Tetrahedron* **2000**, *56*, 1783. (f) Cyrañski, M. K.; Stêpieñ, B. T.; Krygowski, T. M. *Tetrahedron* **2000**, *56*, 9663. (g) Krygowski, T. M.; Cyrañski, M. K. *Chem. Rev*. **2001**, *101*, 1385. (h) Krygowski, T. M.; Cyrañski, M. K.; Anulewicz-Ostrowska, R. *Pol. J. Chem*. **2001**, *75*, 1939.

(28) (a) Schleyer, P. v. R.; Maerker, C.; Dransfeld, A.; Hommes, N. J. R. v. E. *J. Am. Chem. Soc*. **1996**, *118*, 6317. (b) Cyrañski, M. K.; Krygowski, T. M.; Wisiorowski, M.; Hommes, N. J. R. v. E.; Schleyer, P. v. R. *Angew. Chem. Int. Ed. Engl*. **1998**, *37*, 177. (c) Subramanian, G.; Schleyer, P. v. R.; Jiao, H. *Angew. Chem. Int. Ed. Engl*. **1996**, *35*, 2638. (d) Jiao, H.; Schleyer, P. v. R. *Angew. Chem. Int. Ed. Engl*. **1996**, *35*, 2383. (e) Jiao, H.; Schleyer, P. v. R.; Mo, Y.; McAllister, M. A.; Tidwell, T. T. *J. Am. Chem. Soc*. **1997**, *119*, 7075. (f) Schleyer, P. v. R.; Jiao, H.; Hommes, N. J. R. v. E.; Malkin, V. G.; Malkina, O. *J. Am. Chem. Soc*. **1997**, *119*, 12669. (g) Subramanian, G.; Schleyer, P. v. R.; Jiao H. *Organometallics* **1997**, *16*, 2362. (h) Jemmis, E. D.; Kiran, B. *Inorg. Chem*. **1998**, *37*, 2110.

(29) (a) Apeloig, Y.; Arad, D.; Rappoport, Z. *J. Am. Chem. Soc*. **1990**, *112*, 9131. (b) Smith, B. J.; Nguyen, M. T.; Bouma, W. J.; Radom, L. *J. Am. Chem. Soc*. **1991**, *113*, 6452. (c) Lammertsma, K.; Prasad, B. V. *J. Am. Chem. Soc*. **1993**, *115*, 2348. (d) Lammertsma, K.; Prasad, B. V. *J. Am. Chem. Soc*. **1994**, *116*, 642. (e) Harris, N. J.; Lammertsma, K. *J. Am. Chem. Soc*. **1996**, *118*, 8048. (f) Lammertsma, K.; Bharatam, P. V. *J. Org. Chem*. **2000**, *65*, 4662. (g) Wong, W. M.; Wiberg, K. B.; Frisch, M. J. *J. Am. Chem. Soc*. **1992**, *114*, 1645. (h) Long, J. A.; Harris, N. J.; Lammertsma, K. *J. Org. Chem*. **2001**, *66*, 6762. (i) Koskimies, J.; Uggla, R.; Sundberg, M. R. *Acta Chem. Scand*. **1994**, *48*, 417. (j) *The Chemistry of Enols*; Rappaport, Z. Ed.; John Wiley: Chichester, 1990. (k) Bharatam, P. V.; Khanna, S. *J. Phys. Chem*. **2004**, *108*, 3784.

(30) The conversion of isomers **AG3-2** to **AG3** and **AG3-3** to **AG3-1** can take place through the rotational paths involving lower energy requirements than the 1,3-H shift processes, hence the 1,3-H shift processes in these two cases are not expected to take place on the PE surface.